Cent. Eur. J. Phys. • 10(5) • 2012 • 1202-1209
DOI: 10.2478/s11534-012-0136-6

VERSITA

Central European Journal of **Physics**

Microstructural and electrical properties of $Y_{0.07}Sr_{0.93-x}TiO_{3-\delta}$ perovskite ceramics

Research Article

Tadeusz Miruszewski*, Beata Bochentyn, Jakub Karczewski, Maria Gazda, Bogusław Kusz

Faculty of Applied Physics and Mathematics, Gdańsk University of Technology, Narutowicza 11/12, 80-233 Gdansk, Poland

Received 2012 March 20; accepted 2012 September 18

Abstract: In order to find a relationship between electrical and microstructural properties, yttrium-doped strontium titanate (7 mol%) with various values of strontium nonstoichiometry was investigated and shown in this work. It has been observed that yttrium doping can affect the electrical properties of $SrTiO_3$ to a great extent. Moreover, the microstructural and electrical properties can be influenced by strontium nonstoichiometry. The defect chemistry explaining obtained results was also suggested and discussed.

PACS (2008): 81.05.-t, 81.40.-z, 81.70.-g, 81.90.+c, 82.47.-a

Keywords: yttrium-doped strontium titanate • nonstoichiometry • perovskite

1. Introduction

Perovskite-related materials are commonly used in various electrochemical devices and in electronic industry, for example as dielectrics in capacitors, temperature coefficient resistors or piezoelectric transducers [1, 2]. Therefore, much effort needs to be made in order to improve the properties of these structures [3]. One of the most widely used representatives of perovskite materials is strontium titanate ($SrTiO_3$). It has been reported in the literature that it is one of the most promising candidates for anode and cathode materials for Solid Oxide Fuel Cells, because of catalytic and conductivity performance [3, 20]. However, in a pure form strontium titanate is a dielectric material, so it requires some modifications. Electronic conductivity of $SrTiO_3$ can be significantly increased either by reduction at low oxygen partial pressure or by doping with aliovalent ions on the A and/or B site. Donors such as Y^{3+} or La^{3+} on the Sr^{2+} site and Nb^{5+} on the Ti^{4+} site convert $SrTiO_3$ into a highly conducting n-type material [5]. On the other hand acceptor dopants like Al^{3+}, Co^{3+} or Fe^{3+} on Ti^{4+} site allow one to obtain a p-type material [6]. Furthermore, it has been reported that acceptor doping also results in an increased oxygen vacancy concentration and thus an increased ionic conductivity of $SrTiO_3$ [5, 6]. Most of the papers about strontium titanate modifications refer to yttrium doping, because this material has a high total conductivity and its chemical stability is better than these of La-doped strontium titanate [7]. Moreover, the electrical and structural properties of $SrTiO_3$ strongly depend on its defects concentration. There are many scientific groups that investigate the influence of defect chemistry or Sr/Ti stoichiometry on these properties [3, 8]. All equations presented below are written using a Kroger-Vink no-

*E-mail: tadmir1@interia.pl

tation with the following symbols: $[V_O^{**}]$ – concentration of oxygen vacancies, $[V_{Sr}^{''}]$ – concentration of strontium vacancies, $[Y_{Sr}^{*}]$ – donor concentration, $[Ti_{Ti}^{'}]$ – concentration of reduced Ti^{3+} ions and Ti_{Ti}^{x}, O_O^{x}, Sr_{Sr}^{x} symbols denoting ions sitting on lattice site with a neutral charge.

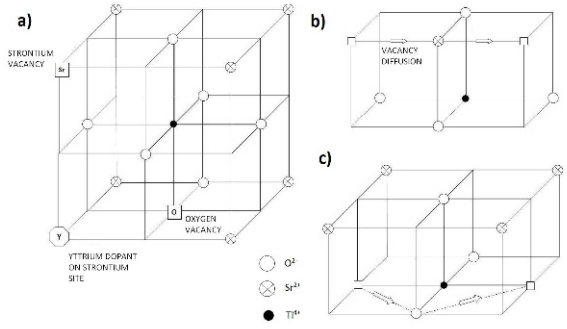

Figure 1. a) Crystal structure of Y-doped $SrTiO_3$ with an illustration of possible paths of migration b) strontium vacancy, c) oxygen vacancy.

In Fig. 1a a crystal structure of Y-doped strontium titanate with a sample of oxygen (V_O^{**}) and strontium ($V_{Sr}^{''}$) intrinsic vacancies is shown. Fig. 1b and Fig. 1c show preferred paths for strontium and oxygen vacancies migration in $SrTiO_3$ structure. It should be noted that the energy of titanium defect ($V_{Ti}^{''''}$) formation is significantly higher than the energy of strontium defect formation [9]. Thus, it seems that Ti vacancies ($V_{Ti}^{''''}$), whose presence is much less probable in the structure, may not be taken into account in defect chemistry of $SrTiO_3$ and are not presented in the picture. In general, both strontium vacancies, oxygen vacancies and yttrium dopants increase the conductivity. The highest contribution to total conductivity of the material show oxygen vacancies.

Generally, for donor doped $SrTiO_3$ ceramics, according to an electroneutrality condition, a sum of positively and negatively charged mobile and immobile species is required. It can be written using a Kroger-Vink notation as follows [10]:

$$n + 2\left[V_{Sr}^{''}\right] = 2\left[V_O^{**}\right] + \left[Y_{Sr}^{*}\right]. \tag{1}$$

In the case of constant value of donors concentration, a number of electrical charge carriers [symbol n in Eq. (1)] depend on the strontium and oxygen vacancies concentration. There exist two alternative mechanisms for oxygen vacancy formation. One of them can be described by Eq. (2):

$$2Ti_{Ti}^{x} + O_O^{x} \Longleftrightarrow 2Ti_{Ti}^{'} + V_O^{**} + \frac{1}{2}O_2(g). \tag{2}$$

This explains the process of oxygen ion release from lattice in a reducing atmosphere. A formation of $[Ti_{Ti}^{'}]$ is related with formation of free charge carriers. So the concentration of reduced Ti^{3+} ions with one delocalizated/free electron depends, in very low partial pressures, on the concentration of yttrium $[Y_{Sr}^{*}]$ and on the oxygen vacancy concentration [8], according to Eq. (3):

$$n = \left[Ti_{Ti}^{'}\right] = 2\left[V_O^{**}\right] + \left[Y_{Sr}^{*}\right]. \tag{3}$$

The second process of oxygen vacancy formation in $SrTiO_3$ perovskite structures, reported by Moos et al. [10], is related to formation of SrO phase, known as Ruddlesden-Popper phase. It has been shown that Schottky-type defects are predominant in this process. The formation of strontium and oxygen vacancies can be explained by Eq. (4), [10]:

$$Sr_{Sr}^{x} + O_O^{x} \Longrightarrow V_O^{**} + V_{Sr}^{''} + SrO. \tag{4}$$

Additionally, Blennow et al. [11] suggest that charge compensation of donor dopants is done mainly by formation of strontium vacancies. In the case of Y-doped $SrTiO_3$, in high oxygen partial pressure, it can be described by reaction (5):

$$\begin{aligned}(1-x)SrO + TiO_2 + \frac{x}{2}Y_2O_3 \\ \Longleftrightarrow \left(1-\frac{3x}{2}\right)Sr_{Sr}^{x} + \frac{x}{2}V_{Sr}^{''} \\ + Ti_{Ti}^{x} + xY_{Sr}^{*} + 3O_O^{x} + \frac{x}{2}SrO.\end{aligned} \tag{5}$$

On the basis of these reactions, donor doping of stoichiometric strontium titanate leads to precipitation of SrO [12]. As it has been mentioned, many scientific groups try to explain the mechanism of defect formation and its influence on the electrical and structural properties (grain sizes, phase composition) of $SrTiO_3$-based structures. For example Blennow et al. [8] showed that electronic conductivity of $SrTiO_3$ is associated with concentration of reduced Ti^{4+} ions [reaction (2)]. The group of Baurer et al. [3] investigated nonstoichiometric strontium titanate and reported that an excess of TiO_2 in the structure results in a formation of strontium and oxygen vacancies, even in oxygen atmosphere, according to Eq. (6):

$$\begin{aligned}nSrTiO_3 + TiO_2 \Longleftrightarrow nSrTiO_3 + Ti_{Ti}^{x} + 2O_O^{x} \\ + V_{Sr}^{''} + V_O^{**}.\end{aligned} \tag{6}$$

Simultaneously, it was shown by Blennow et al. [12] that Sr excess is accommodated in SrO phase. Gomann et al.

[13] reported also that diffusion of Sr and Ti cation takes place generally through strontium vacancies.

The influence of defect chemistry on ionic conductivity of $SrTiO_3$ was studied by Zhao et al. [6]. The authors suggest a new defect analysis of Y-doped strontium titanate with strontium deficiency. According to Zhao et al. [6], this structure can form oxygen vacancies both by reactions written in Eqs. (4) and (7):

$$2Y_{Sr}^{*} + 3O_O^{x} \Longrightarrow 2V_{Sr}^{''} + 3V_O^{**} + Y_2O_3\,. \qquad (7)$$

According to Eq. (7) and to the electroneutrality condition (1), a decrease of yttrium concentration and increase of strontium and oxygen vacancies concentration results in a decrease of free charge carriers concentration and, at the same time, in a decrease of electronic conductivity. However, A-site deficiency in $SrTiO_3$ ceramic has also a great influence on ionic conductivity, caused by the increase of oxygen vacancies concentration [6]. Gao et al. [14] suggest that B-site deficiency is generating oxygen vacancies, and for charge compensation, the decrease of Ti^{3+} ion concentration occurs. But this theory indicates the existence of titanium vacancies, what disagrees with thermodynamic calculations [15]. Astala et al. [15] reported that the energy of strontium vacancy formation is about 4 times lower than the energy of titanium defect formation. Thus, in this paper we will base our explanations on a conception of nonstoichiometry present in Sr-site, not in Ti-site.

In this paper, the influence of A-site nonstoichiometry in the $Y_{0.07}Sr_{0.93}TiO_{3-\delta}$ composition on its structural and electrical properties was investigated and confronted with previously reported papers [6–8, 11, 14, 17]. There are some reports about the solubility limit of yttrium in $SrTiO_3$ [7]. For example, above the 8 wt% of yttrium in A-site, the insulating $Y_2Ti_2O_7$ phase can be observed and the material is not single-phase. On the basis of literature reports a 7 wt% of yttrium doping into strontium titanate structure has been choosen in this paper. The most possible defect formation processes and charge compensation in $Y_{0.07}Sr_{0.93}TiO_{3-\delta}$ structure was examined and discussed.

2. Experimental

Yttrium-doped strontium titanate with different values of A-site deficiency ($Y_{0.07}Sr_{0.93-x}TiO_{3-\delta}$; $x = -0.05; 0; 0.05$) was prepared via conventional solid-state reaction method from Y_2O_3 (Sigma Aldrich, 99,9%), TiO_2 (Sigma Aldrich, 99%) and $SrCO_3$ (Sigma Aldrich,98%). It has been previously shown [7], that 7 mol% is an optimal amount of Y doping at Asite, and allows to get phase-pure material. After ball-milling for 12 h using ZrO_2 balls, the mixture was calcined at 1200°C for 12 h, and then at 1400°C for 12 h in air. To improve the electrical properties, samples of YSTO ceramics were reduced at 1400°C for 10 h in dry hydrogen.

The phase composition of bulk samples sintered in air and reduced in hydrogen was analyzed by the X-ray diffraction method by the X-Pert Pro MPD Philips diffractometer using Cu Kα (1.542 Å) radiation at room temperature. The XRD patterns were also analyzed by the Rietveld refinement method using a X'Pert Plus program with the pseudo-Voigt profile function applied. The Phenom G2 Pro scanning electron microscope (SEM) was used to analyze the morphology of samples. The densities and porosities of samples were measured using Archimedes method using kerosene as a liquid medium.

Temperature dependence of conductivity was studied by DC two-wire (2W) and DC four-wire (4W) method for the samples before and after reduction, respectively. Impedance spectroscopy measurements of reduced samples were carried out at 800°C in a self-made cell. Measurements were performed using Solartron 1260 frequency response analyzer. An excitation voltage of amplitude 10 mV was applied and the frequency was set from 4 MHz to 1 kHz.

In order to avoid writing a long stoichiometric formula in the Results and Discussion section, some abbreviations have been used for all investigated compositions. They are listed in Tab. 1.

Table 1. Abbreviations of $Y_{0.07}Sr_{0.93-x}TiO_{3-\delta}$ (where x ϵ ⟨-0.05;0.05⟩) ceramics investigated in this study.

x in $Y_{0.07}Sr_{0.93-x}TiO_{3-\delta}$	Composition	Abbreviation
0.05	$Y_{0.07}\ Sr_{0.88}TiO_{3-\delta}$	YST88O
0	$Y_{0.07}\ Sr_{0.93}TiO_{3-\delta}$	YSTO
-0.05	$Y_{0.07}\ Sr_{0.98}TiO_{3-\delta}$	YST98O

3. Results and discussion

3.1. Microstructural properties

The X-ray diffraction patterns of samples sintered in air are shown in Fig. 2, whereas those which were additionally reduced at 1400°C for 10 h in hydrogen are shown in Fig. 3.

The corresponding results of quantitative analysis for the same compositions are presented in Tab. 2.

On the basis of the obtained data it can be concluded that compounds differ from each other significantly, depending on the composition and heat treatment conditions. In both

Table 2. Results of quantitative analysis of XRD data obtained from samples before and after reduction at 1400°C for 10 h in H_2; accuracy: $\delta m/m = \pm 1\%$.

Compound	YST88O		YSTO		YST98O	
weight content of phase [%]	Before reduction	After reduction	Before reduction	After reduction	Before reduction	After reduction
$SrTiO_3$	91	97	94	98	93	98
$Y_2Ti_2O_7$	6	3	6	2	0	0
TiO_2	3	0	0	0	0	0
SrO	0	0	0	0	7	0
Y_2O_3	0	0	0	0	0	2

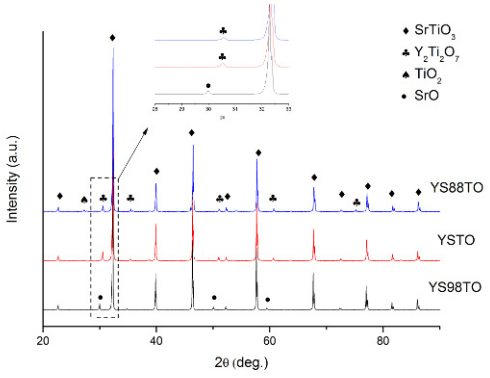

Figure 2. XRD patterns of YS88TO, YSTO and YS98TO compounds synthesized in air.

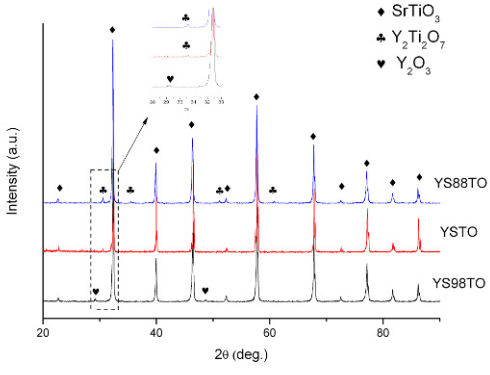

Figure 3. XRD patterns of YS88TO, YSTO and YS98TO compounds reduced at 1400°C for 10 h in H_2.

nonreduced and reduced Sr-deficient samples (YS88TO) a small amount of $Y_2Ti_2O_7$ (pyrochlore) phase is present. In addition, a 3 wt% of TiO_2 called Magneli phase can be found in nonreduced YS88TO composition. It appears to be decomposed during the process of high temperature reduction according to the Eq. (6) and TiO_2 reflexes are not seen in XRD data of reduced YS88TO. The amount of $Y_2Ti_2O_7$ phase is also partially decreased from 6% to 3% during reduction in low oxygen partial pressure. We suggest that yttrium from pyrochlore may compensate additional strontium vacancies ($V_{Sr}^{''}$) formed in reducing conditions (1), whereas the residual TiO_2 may be decomposed as shown in (6). The analogical discussion may be performed in reference to stoichiometric composition YSTO. In both non-reduced and reduced samples a small amount of pyrochlore phase can be found, however it decreases from 6 to 2 wt% after reduction in low oxygen partial pressure as a result of the same mechanism that was suggested for Sr-deficient compound. The strontium excess in the structure (YS98TO) assits in? the formation of SrO Ruddlesden-Popper (RP) phase. Before reduction its amount was identified at the level of 7 wt%, whereas after reduction it disappeared and a trace amount of Y_2O_3 phase was found. A complete SrO disappearance results from the fact that during reduction both oxygen vacancies (V_O^{**}) and strontium vacancies ($V_{Sr}^{''}$) are formed in order to satisfy the electroneutrality condition (1). The latter may accommodate strontium from RP phase that may explain why there is no SrO in the XRD patterns for YS98TO. On the other hand, the appearance of a trace amount of Y_2O_3 in YS98TO composition also need some explanation. As the amount of strontium vacancies is limited in the structure, they can not be further formed in order to compensate the additional charge from donor dopant [$Y_{Sr}^{\cdot}$] and thus to provide a full incorporation of yttrium to the lattice. Consequently, a trace amount of Y_2O_3 may be formed, as it was shown by Zhao et al. [6] in Eq. (7). It is observed only in the reducing conditions when oxygen vacancies (V_O^{**}) are formed. Results of Rietveld analysis performed for non-reduced and reduced samples are presented in Fig. 4. It shows that unit cell parameters of all reduced compounds are higher than those of non-reduced samples. It results from the presence of Ti^{3+} ion that has a bigger ionic radius (0.67 Å) [16] than the ionic radius of Ti^{4+} (0.605 Å) [16]. As a consequence, it causes the expansion of the cell, regardless of the stoichiometry of each compound. Furthermore, the A-site nonstoichiometry influences the lattice parameters of Y-doped $SrTiO_3$. As

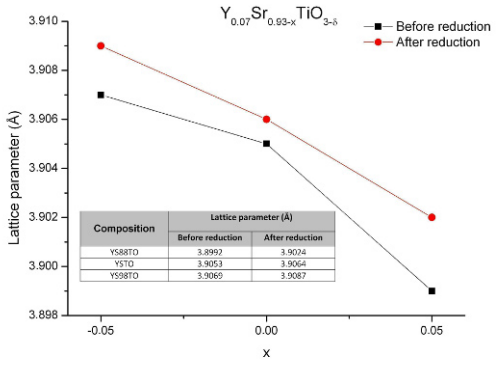

Figure 4. Unit cell parameters $a = b = c$ [Å] of perovskite $SrTiO_3$ phase of $Y_{0.07}Sr_{0.93-x}TiO_{3-\delta}$ samples synthesized in air (squares) and reduced at 1400°C for 10 h in H_2 (circles); accuracy: 10^{-3} Å. The solid line is a guide for the eye only.

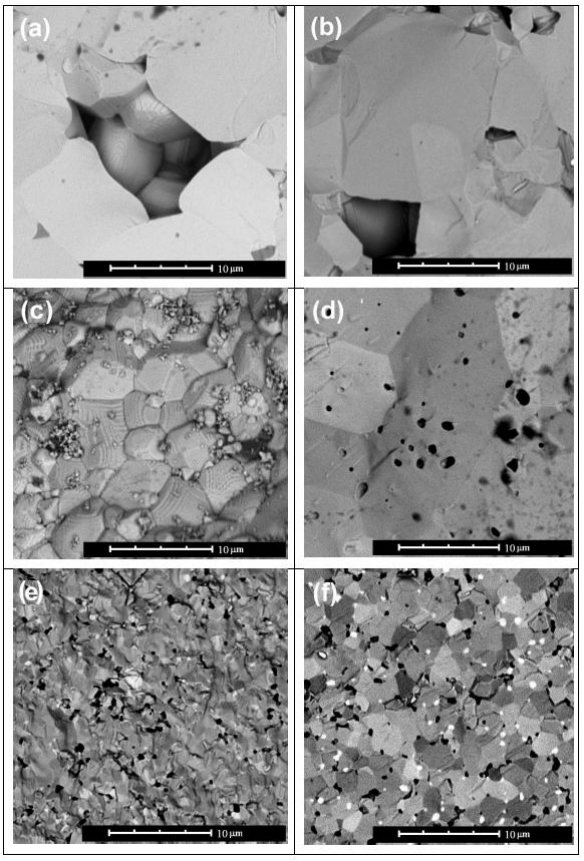

Figure 5. SEM images of fractured cross sections of YS88TO (a), YSTO (c) and YS98TO (e) compounds synthesized in air and YS88TO (b), YSTO (d) and YS98TO (f) compounds reduced at 1400°C for 10 h in H_2. There is 10000× magnification presented for each composition.

shown in Fig. 4, the A-site excess (YS98TO) results in the expansion of the unit cell compared to the stoichiometric (YSTO) and A-deficient (YS88TO) compositions. These observations are in good agreement with the reports of Ma et al. [17] and Gao et al. [14]. Ma et al. [17] suggest that the bigger unit cell of A-site excess compound results from the presence of Y_2O_3 impurity. If fewer Sr^{2+} ions (1.44 Å) [16] are replaced by smaller Y^{3+} (1.019 Å) [16] ions, it can lead to larger lattice parameters than in the case of A-site deficient samples. This corresponds well with our experimental results. The SEM images of fractured cross sections of all investigated compositions are shown in Figs. 5a, c, e (non-reduced samples) and Figs. 5b, d, f (reduced samples). These pictures confirm that there is a significant difference in microstructure depending on samples composition and preparation conditions (reduced or not). In a group of non-reduced pellets, those with A-site deficiency (YS88TO) have the largest grains (5-10 mm) with sharply outlined grain boundaries. An average grain size of the stoichiometric compound (YSTO) is twice as small as that of YS88TO. Some randomly distributed nanometre size grains can be found in Fig. 5c. In the case of A-site excess composition (YS98TO) it is difficult to distinguish grain boundaries because the grains are much smaller than those previously discussed (below 1 mm). A similar phenomenon of grain growth with decreasing strontium content can be observed for samples that were reduced at 1400°C for 10 h in hydrogen (Figs. 5b, d, f). Nevertheless, the grains of stoichiometric (YSTO) and A-site excess (YS98TO) compounds are bigger than those of corresponding non-reduced compositions. Moreover, the reduced samples are denser that non-reduced ones. It may be suggested, that a grain growth kinetics is limited by SrO Ruddlesden-Popper phases that are present in the structure in a form of intergrowth layers [19]. If there is no SrO in the structure, as it was observed for A-site deficient sample (YS88TO), the grains are big, regardless of the heating atmosphere (Figs. 5a and b). On the other hand, if SrO is present in the structure (non-reduced YS98TO), the grains are very small (Fig. 5e). However, they grow after reduction in hydrogen (Fig. 5f), because strontium from Ruddlesden-Popper phase is accommodated by strontium vacancies ($V_{Sr}^{''}$). This phenomenon of enhanced grain growth after reduction is also visible in the case of stoichiometric compound (YSTO). Although no evidence of SrO was found in this sample, we suggest that a trace amount of this phase can be formed according to Eq. (5), as it was reported by Blennow et al. [11]. It can not be identified with XRD technique because of its limited sensitivity, but it may influence the grain growth kinetics and thus it can explain our SEM observations.

3.2. Electrical properties

The results of two-probe direct current conductivity measurements of YS88TO, YSTO and YS98TO samples sintered at 1400°C for 12 h in air are shown in Fig. 6. The same temperature dependence of conductivity was

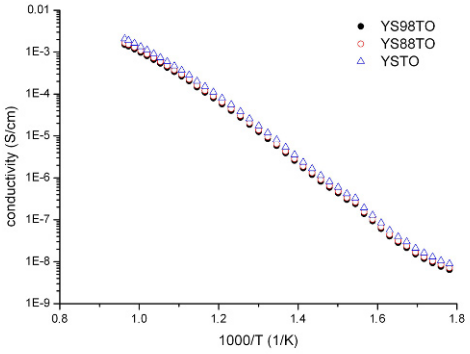

Figure 6. Electrical conductivity plot of Y-doped $SrTiO_3$ bulk samples synthesized at 1400°C for 12 h in air.

observed for all investigated samples. A semiconducting like behavior was also observed for all samples and a very low value of maximum total conductivity (around 5×10^{-3} S/cm) was noticed for this compounds. In order to explain this phenomenon it should be remembered that in the case of non reduced samples free charge carriers are generally formed because of donor doping. Concentration of oxygen vacancies, which are i.a. responsible for electrical conductivity, is at high oxygen partial pressure significantly lower than at low oxygen partial pressure. Then, this low value of conductivity may occur because of low oxygen vacancies concentration and, in consequence, because of lower total concentration of free charge carriers, according to Eq. (3).

The temperature dependence of conductivity for three samples reduced in hydrogen atmosphere with different values of Sr-site nonstoichiometry is presented in Fig. 7. A significant increase of total conductivity compared to conductivity of non-reduced samples was noticed. According to Blennow et al. [11] oxygen has a tendency to leave lattice at low oxygen partial pressure [$p(O_2) \approx 10^{-18}$]. Thus the concentration of oxygen vacancies significantly increases. Consequently, the amount of free charge carriers also increases, as described in Eq. (3). As presented in Fig. 5, the total conductivity at 700°C was noted for YS98TO, YS88TO, YSTO around 10 S/cm, 40 S/cm, 100 S/cm, respectively. Moreover, a semiconducting-like to metal-like behavior transition, typical for doped $SrTiO_3$, was observed for all samples:

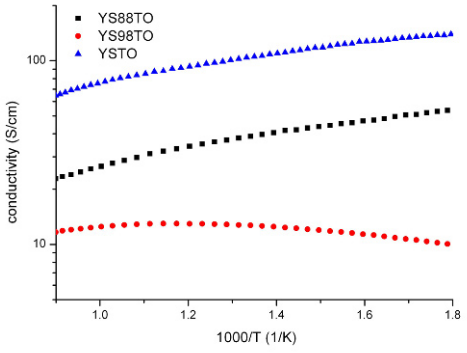

Figure 7. Electrical conductivity plot of Y-doped $SrTiO_3$ bulk samples with various stoichiometry reduced at 1400°C for 10 h in H_2.

at around 500°C for YSTO, 400°C for YS88TO and 900°C for YS98TO sample. Thus, the process of transition to metal-like behavior, required for a good anode material, takes place in the lowest temperature for YS88TO sample. Besides, it has been observed that there is a strong influence of nonstoichiometry in a Sr-site on a total conductivity value. The observed differences between samples may be explained by a defect chemistry of nonstoichiometric donor doped strontium titanate, described in the introduction. In stoichiometric Y-doped $SrTiO_3$, the concentration of free charge carriers depends on dopants level in A-site and on oxygen vacancies concentration, which can be increased under reducing conditions (3).

For YS88TO sample (with strontium deficiency) more $Y_2Ti_2O_7$ phase was observed in the XRD pattern (Fig. 3) than in the stoichiometric composition. Most probably dielectric character of pyrochlore phase causes that a total conductivity of YS88TO is lower in relation to YSTO. Furthermore, the formation of pyrochlore phase can result in a removal of yttrium from strontium lattice and, in consequence, in a decrease of donors concentration. It can be schematically described as follows:

$$Y_2Ti_2O_7\text{excess} \longrightarrow \left[\text{dec.}\left(Y_{Sr}^{*}\right)\right] \longrightarrow [\text{dec.n}] \qquad (8)$$

where [dec.(Y_{Sr}^{*})] denotes a decreased yttrium dopants part caused by a pyrochlore formation and [dec.n] designates a total conductivity decrease. This hypothesis may explain a lower level of total conductivity of YS88TO than in the case of the stoichiometric sample YSTO. On the basis of these considerations it can be suggested that a strontium deficiency does not indicate a formation of strontium vacancies, which influence oxygen vacancies concentration and conductivity growth. In the case of sam-

ple with Sr excess in the structure (YS98TO), some amount of SrO Ruddlesden-Popper phase is formed (4). According to Eq. (5) the excess of SrO phase causes a reduction of strontium vacancies. It leads to simultaneous reduction of oxygen vacancies concentration, which are generally responsible for free charge carriers formation. This process can be schematically described as:

$$\mathrm{SrOexcess} \Longrightarrow \left[\mathrm{dec.}\left(V_{Sr}^{''}\right)\right] \Longrightarrow \left[\mathrm{dec.}\left(V_{O}^{**}\right)\right] \Longrightarrow [\mathrm{dec.n}] \quad (9)$$

where $[\mathrm{dec.}(V_{Sr}^{''})]$ denotes a decreased strontium vacancy concentration, $[\mathrm{dec.}(V_{O}^{**})]$ designates a decrease of oxygen vacancies concentration and [dec.n] denotes the total conductivity decrease. On the other hand, it can be suggested that there may also be an additional process leading to a total conductivity decrease in YS98TO sample. Because there are less strontium vacancies, there has to be less yttrium in the lattice. That leads to Y_2O_3 phase appearance, shown also in the XRD pattern (Fig. 3). The increase in the amount of Y_2O_3 results in a decrease of donor concentration, so the total conductivity may be lower, according to the explanation of Zhao et al. [6]. In summary, it can be stated that there are two possible reasons of total conductivity decrease: excess of SrO phase and Y_2O_3 appearance in the structure. These reasons may explain why the YS98TO sample has the lowest conductivity from all investigated samples.

In order to find a relationship between electrical properties and microstructure, the impedance spectra of nonstoichiometric YS88TO and YS98TO samples were compared. The impedance spectra obtained at 800°C in air is presented in Fig. 8. The equivalent electrochemical circuit for a typical polycrystalline ceramics composed of two series systems, resistor in parallel with a constant phase element (CPE), is presented in the same figure (Fig. 8). The high-frequency semicircle (marked as HF) describes a resistance of the bulk of polycrystalline specimen, whereas the other one (marked as LF) represents highly resistive grain boundaries. The resistivity of high and low frequency semicircles and area specific resistivity ASR_{LF+HF} were calculated and compared for two investigated samples. It was found that ASR_{LF+HF} for both YS98TO and YS88TO samples is comparable (around 350 Ω cm). Thus, the influence of Sr nonstoichiometry can not be identified by the impedance spectroscopy measurements of donor-doped $SrTiO_3$. That leads to a conclusion that a relationship between microstructure of Y-doped $SrTiO_3$ and its electrical properties cannot be seen on impedance spectra. However, it does not correspond with the results of DC fourprobe measurement, where some differences depending on composition were noticed. For example, samples with strontium excess have lower concentrations of strontium and oxygen vacancies, which results in a lower conductivity. In the case of samples with a strontium deficiency a pyrochlore phase precipitates and the donor concentration also decreases resulting in a lower conductivity. However, in general strontium deficiency does not change the oxygen and strontium vacancy concentrations. This mismatch between the results of AC and DC measurements can be explained by the fact that ASR_{LF+HF} describes a sum of all features and phenomena taking place in an investigated sample, whereas the temperature dependence of resistivity shows just a sum of ionic and electronic conductivity, which is only one factor affecting the value of ASR_{LF+HF}. We suggest that the electrical properties are mainly determined by defect chemistry, while modifications of microstructure play the minor role.

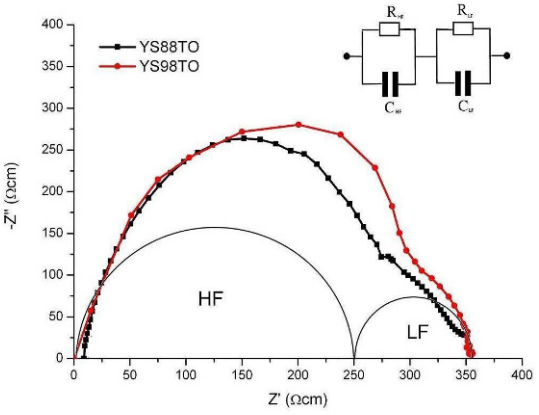

Figure 8. Impedance diagram of $Y_{0.07}Sr_{0.93-x}TiO_{3-\delta}$ reduced ceramics with different values of stoichiometry measured in 800°C. Thin solid line shows Nyquist plot for ideal electrical equivalent circuit. In the corner: electrical equivalent circuit.

4. Conclusions

The electrical and microstructural properties of $Y_{0.07}Sr_{0.93-x}TiO_{3-\delta}$ for different values of x were characterized and shown in this work. The stoichiometry of Sr-sites has a great influence on all these properties. The samples sintered at 1400°C for 12 h in air presented insufficient conductivity (around 5×10^{-3} S/cm at 1000°C) for IT-SOFC anode application. Therefore reduction in low oxygen partial pressure conditions was required. After this process, total electrical conductivity significantly increased and it was the highest for the stoichiometric ($x = 0$) sample (100 S/cm at 700°C). Also the microstructure of $Y_{0.07}Sr_{0.93-x}TiO_{3-\delta}$ strongly depended on Sr-site

nonstoichiometry, which was put forward on XRD and SEM figures. Additionally, SrO, Y_2O_3 and $Y_2Ti_2O_7$ insulating phases, typical of nonstoichiometric Y-doped $SrTiO_3$ structures, have been observed. It has also been suggested, according to impedance spectroscopy results, that there is no significant relationships between microstructure and electrical properties. The explanations of the stoichiometry influence on those properties basing on defect chemistry were discussed and compared with other papers.

Acknowledgments

The authors would like to acknowledge D.Sc. P. Jasiński and all people not mentioned in author list for providing us a good suggestions and facilities to complete this paper.

References

[1] Q. Ma, F. Tietz, A. Leonide, E. Ivers-Tiffe, J. Power Sources 196, 7308 (2010)
[2] N.Q. Minh, J. Am. Ceram. Soc. 76, 563 (1993)
[3] M. Baurer, H. Kungl, M.J. Hoffmann, J. Am. Ceram. Soc. 92, 601 (2009)
[4] O.A. Marina, N.L. Canfield, J.W. Stevenson, Solid State Ionics 149, 21 (2002)
[5] S. Hui, A. Petric, Mat. Res. Bulletin 37, 1215 (2002)
[6] H. Zhao, F. Gao, X. Li, C. Zhang, Y. Zhao, Solid State Ionics 180, 193 (2009)
[7] X. Huang, H. Zhao, W. Shen, W. Qiu, W.Wu, J. Phys. Chem. Solids 67, 2609 (2006)
[8] P. Blennow, K.K. Hansen, L.R. Wallenberg, M. Mogensen, Electrochim. Acta 52, 1651 (2006)
[9] J. Crawford, P. Jacobs, J. Solid State Chem. 144, 423 (1999)
[10] R. Moos, K.H. Hardtl, J. Am. Ceram. Soc. 80, 2549 (1997)
[11] P. Blennow, A. Hagen, K.K. Hansen, L.R. Wallenberg, M. Mogensen, Solid State Ionics 179, 2047 (2008)
[12] S.N. Ruddlesden, P. Popper, Acta Crystallogr. A 11, 54 (1958)
[13] K. Gomann, G. Borchart, A. Gunhold, W. Maus-Friedrichs, H. Baumann, Phys. Chem. Chem. Phys. 6, 3639 (2004)
[14] F. Gao, H. Zhao, X. Li, Y. Cheng, X. Zhou, F. Cui, J. Power Sources 185, 26 (2008)
[15] R. Astala, P.D. Bristowe, Comp. Mater. Sci. 22, 81 (2001)
[16] R.D. Shannon, Acta Crystallogr. A 32, 751 (1976)
[17] Q. Ma, F. Tietz, D. Stöver, Solid State Ionics 192, 535 (2011)
[18] W. Menesklou, H.-J. Schreiner, K.H. Härdtl, E. Ivers-Tiffée, Sensor. Actuat. B-Chem. 59, 184 (1999)
[19] U. Balachandran, N.G. Eror, J. Mater. Sci. 17, 2133 (1982)
[20] S. Molin, W. Lewandowska-Iwaniak, B. Kusz, M. Gazda, P. Jasiński, J. Electroceram. 28, 80 (2012)